BIOMOLECULES & THERAPEUTICS

Original Article
Biomol Ther 27(4), 381-385 (2019)

4'-O-β-D-Glucosyl-5-O-Methylvisamminol Attenuates Pro-Inflammatory Responses and Protects against Oxidative Damages

Ok-Kyung Yoo and Young-Sam Keum*

Integrated Research Institute for Drug Development, College of Pharmacy, Dongguk University, Goyang 10326, Republic of Korea

Abstract

We attempted to examine anti-inflammatory and anti-oxidant effects of 4'-O-β-D-glucosyl-5-O-methylvisamminol (GOMV), the first epigenetic inhibitor of histone phosphorylation at Ser10. While GOMV did not affect the viability of murine macrophage RAW 264.7 cells, it significantly suppressed lipopolysaccharide (LPS)-induced generation of prostaglandin E_2 (PGE_2) and nitric oxide (NO) through transcriptional inhibition of cyclooxygenase-2 (COX-2) and inducible nitric oxide synthase (iNOS). GOMV also scavenged free radicals *in vitro*, increased NF-E2-related factor 2 (NRF2), and activated antioxidant response element (ARE), thereby resulting in the induction of phase II cytoprotective enzymes in human keratinocyte HaCaT cells. Finally, GOMV significantly protected HaCaT cells against 12-*O*-tetradecanoylphorbol-13-acetate (TPA)-induced oxidative intracellular damages. Together, our results illustrate that GOMV possesses anti-inflammatory and anti-oxidant activity.

Key Words: 4'-O-β-D-glucosyl-5-O-methylvisamminol (GOMV), Reactive oxygen species (ROS), NF-E2-related factor 2 (NRF2), Antioxidant response element (ARE)

INTRODUCTION

Exogenous and endogenous ROS (reactive oxygen species) impart significant oxidative damages on human keratinocytes (Schieber and Chandel, 2014). To counteract oxidative stress, organisms possess diverse anti-oxidant proteins, including NF-E2-related factor 2 (NRF2) (Itoh *et al*., 1997). Under basal condition, NRF2 is sequestered by Kelch-like ECH-associated protein 1 (KEAP1) in the cytosol and constitutively targeted for poly-ubiquitination. In response to oxidative stress, NRF2 translocates into the nucleus, binds to the antioxidant response element (ARE), and induces the expression of phase II cytoprotective enzymes (Kundu and Surh, 2008). At present, NRF2 is considered as a master regulator of drug metabolism, differentiation, proliferation, and inflammation (Ma, 2013).

Histone H3 phosphorylation at Ser10 and Ser28 is responsible for cell cycle progression during mitosis and transcriptional activation of pro-inflammatory genes during interphase (Baek, 2011). We have reported that transcriptional activation by histone H3 phosphorylation at Ser10 and Ser 28 occurs through recruitment of 14-3-3ε and cyclin-dependent kinase 9 (CDK9) in the promoter of pro-inflammatory genes (Keum *et al*., 2013). In addition, we have reported that 4'-O-β-D-glucosyl-5-O-methylvisamminol (abbreviated as GOMV, Fig. 1A) is the first epigenetic natural compound that interferes with the interaction between histone H3 phosphorylation at Ser10 and 14-3-3ε (Kang *et al*., 2014).

In the present study, we have evaluated anti-inflammatory and anti-oxidant effects of GOMV. More specifically, we sought to investigate whether GOMV could inhibit lipopolysaccharide (LPS)-induced pro-inflammatory responses in murine macrophage RAW 264.7 cells. We also investigated whether GOMV could directly scavenge free radicals *in vitro* and protect human keratinocyte HaCaT cells against 12-*O*-tetradecanoylphorbol-13-acetate (TPA)-induced oxidative damages through induction of NRF2/ARE.

MATERIALS AND METHODS

Cell culture, chemicals, plasmids, and antibodies

GOMV was purchased from Toronto Research Chemicals (North York, ON, Canada). GOMV was dissolved in dimethyl

Open Access https://doi.org/10.4062/biomolther.2018.232

Received Dec 12, 2018 **Revised** Feb 17, 2019 **Accepted** Mar 4, 2019
Published Online Apr 10, 2019

***Corresponding Author**
E-mail: keum03@dongguk.edu
Tel: +82-31-961-5215, Fax: +82-31-961-5206

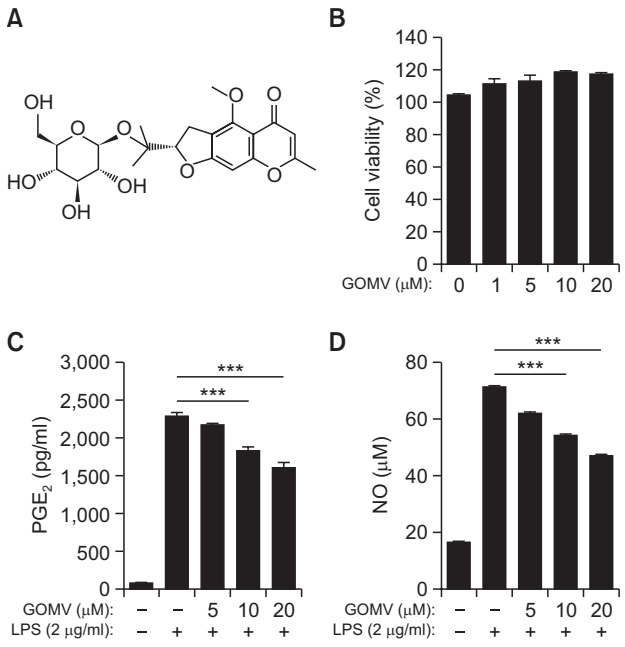

Fig. 1. GOMV suppresses the production of pro-inflammatory cytokines in RAW 264.7 cells. (A) Chemical structure of GOMV. (B) GOMV does not affect the viability of RAW 264.7 cells. Cell viability was measured by MTT assay. (C) GOMV inhibits LPS-mediated generation of PGE_2 in RAW264.7 cells. Asterisks indicate statistical significance with ***p<0.01. (D) GOMV inhibits LPS-mediated production of NO in RAW264.7 cells. Asterisks indicate statistical significance with ***p<0.01.

sulfoxide (DMSO) (vehicle) and used in all *in vitro* experiments at a dilution ratio of 1/1000. LPS and TPA were purchased from Sigma (St. Louis, MO, USA). Dulbelco's modified Eagle's media (DMEM), Roswell Park Memorial Institute (RPMI) media, feral bovin serum (FBS), and penicillin/streptomycin (Pen/Strep) were purchased from WELGENE (Daegu, Korea). RAW 264.7 cells and HaCaT cells were purchased from Korean Cell Line Bank (Seoul, Korea). They were maintained in RPMI media supplemented with 10% FBS and Penicillin/Streptomycin (100 U/ml). Polyclonal antibodies against NRF2, total actin, and 8-hydroxy-2'-deoxyguanosine (8-OH-dG) were purchased from Santa Cruz biotechnology (Santa Cruz, CA, USA). 4-hydroxynonenal (4-HNE) antibody was purchased from Abcam (Cambridge, MA, USA). 2',7'-dichlorofluorescin diacetate (DCF-DA) was purchased from Thermo Fisher Scientific (Waltham, MA, USA).

DPPH and ABTS assay

2,2'-diphenylpicrylhydrazyl (DPPH) was purchased from Cayman (Ann Arbor, MI, USA). 2,2'-azinobis diammonium salt (ABTS) was purchased from Roche Diagnostics (Mannheim, Germany). DPPH and ABTS assays were conducted as described previously (Kim *et al*., 2002, 2003).

MTT assay

Cells were seeded into 96-well plates at density of 3×10^4 cells/well and exposed to GOMV for 24 h. After washing with 1x PBS, cells were incubated with 100 μl 3-(4,5-dimethyl-2-thiazolyl)-2,5-diphenyl-2H-tetrazolium bromide (MTT) solution (10 mg/ml) for 4 h and incubated with 100 μl DMSO. The resulting absorbance was measured at wavelength of 560 nm using a spectrophotometer.

Table 1. List of primers used for real-time PCR

Gene		Primer Sequence
HO-1	Forword	5'-ATGCCCCAGGATTTGTCAGA-3'
	Reverse	5'-ACCTGGCCCTTCTGAAAGTT-3'
NQO1	Forword	5'-ATGGAAGAAACGCCTGGAGA-3'
	Reverse	5'-TGGTTGTCAGTTGGGATGGA-3'
GCLC	Forword	5'-CATTGATTGTCGCTGGGGAG-3'
	Reverse	5'-CTGGGCCAGGAGATGATCAA-3'
GAPDH	Forword	5'-CACAGTCCATTTGCCATCACTG-3'
	Reverse	5'-GTCCACCACTGACACGTTG-3'

Measurement of prostaglandin E_2 (PGE_2) and nitric oxide (NO)

Levels of PGE_2 and NO were measured using PGE_2 ELISA kit (Cayman) and nitric oxide detection kit (INTRON, Seoul, Korea), respectively.

Western blot analysis

After chemical treatment, cells were collected and washed with ice-cold 1x PBS buffer. Cells were lysed with RIPA lysis buffer [50 mM Tris-HCl at pH 8.0, 150 mM NaCl, 1% NP-40, 0.5% deoxycholic acid, 0.1% sodium dodecyl sulfate (SDS), 1 mM Na_3VO_4, 1 mM dithiothreitol (DTT), 1 mM phenylmethylsulfonyl fluoride (PMSF)] on ice for 30 min. Cell lysates were collected by centrifugation and protein concentration was measured using BCA Protein Assay Kit (Thermo Fisher Scientific). Equal amounts of cell lysates were resolved by sodium dodecyl sulfate-polyacrylamide gel electrophoresis (SDS-PAGE) and transferred to polyvinylidene fluoride (PVDF) membranes. After 1 h of incubation in blocking buffer (5% skin milk in 1x PBST) at room temperature, the membrane was incubated with appropriated primary antibodies overnight at 4°C. After washing with 1x PBST three times, the membrane was incubated with horseradish peroxidase (HRP)-conjugated secondary antibodies (Thermo Fischer Scientific). After washing with 1x PBST three times, membranes were finally visualized by enhanced chemiluminescence (ECL) detection system.

Real-time reverse transcription-polymerase chain reaction (RT-PCR)

After treatment, cells were collected and total RNAs were extracted using Hybrid-R RNA extraction kit (GeneAll, Seoul, Korea). Total RNA was subject to cDNA synthesis using PrimeScript RT-PCR kit (TAKARA Korea, Seoul, Korea). Real-time RT-PCR analysis was performed using SYBR mix on a CFX384 Real-time system (BioRad, Hercules, CA, USA). Amplification protocol for PCR was: a single cycle at 95°C for 5 min, 40 cycles of 95°C for 10 s, 59°C for 10 s, and 72°C for 20 s, and a final cycle at 95°C for 10 s. Real-time PCR primers used in the present study are listed in Table 1. The mRNA level of individual genes was normalized to that of glyceraldehyde 3-phosphate dehydrogenase (GAPDH).

Measurement of intracellular reactive oxygen species (ROS)

Intracellular ROS level was measured by DCF-DA stain-

ing followed by observation under a fluorescent microscope. HaCaT cells grown on glass slides were stained with DCF-DA for 30 min. After washing with 1x PBS, fluorescent signals were obtained with a C2 confocal microscope (Nikon Korea, Seoul, Korea). The final image was captured with 400x amplification.

Measurement of luciferase activity

We have established HaCaT-ARE-GFP-luciferase cells by lentiviral transduction as described previously (Lee *et al*., 2018). HaCaT-ARE-GFP-luciferase cells were seeded into 24-well culture plates at density of 2×10^5 cells/well and exposed to GOMV for 24 h. After washing with 1x PBS three times, HaCaT-ARE-GFP-luciferase cell lysates were collected using luciferase lysis buffer [0.1 M potassium phosphate buffer at pH 7.8, 1 % Triton X-100, 1 mM DTT, 2 mM EDTA] for 30 min followed by centrifugation. Luciferase activity was measured with a GLOMAX Multi-system (Promega, Madison, WI, USA) and normalized by protein concentration.

Statistical analysis

Statistical analysis was conducted with Student's *t*-test with at least 5 samples per group.

RESULTS

GOMV suppresses LPS-induced pro-inflammatory responses in RAW 264.7 cells

After treatment of GOMV at different concentrations, we measured the viability of murine macrophage RAW 264.7 cells by MTT assay. Our results show that GOMV did not affect the viability of RAW 264.7 cells (Fig. 1B). We next examined whether GOMV could inhibit LPS-induced pro-inflammatory responses. Our results show that GOMV suppressed LPS-induced generation of pro-inflammatory cytokines such as prostaglandin E_2 (PGE_2) (Fig. 1C) and nitric oxide (NO) in RAW 264.7 cells (Fig. 1D). GOMV also suppressed LPS-induced cyclooxygenase-2 (COX-2) and inducible nitric oxide synthase (iNOS) in RAW 264.7 cells (Fig. 2A). Real-time RT-PCR analysis showed that GOMV suppressed LPS-induced cyclooxygenase-2 (COX-2) (Fig. 2B) and inducible nitric oxide synthase (iNOS) (Fig. 2C) at transcriptional level in RAW 264.7 cells. Taken together, our results demonstrate that GOMV exhibits anti-inflammatory effects on macrophages by suppressing transcription of pro-inflammatory genes.

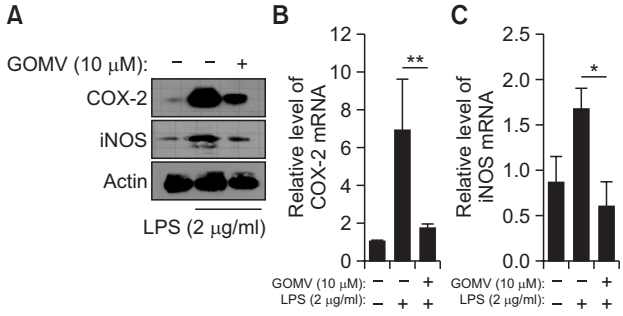

Fig. 2. GOMV transcriptionally inhibits LPS-induced COX-2 and iNOS in RAW 264.7 cells. (A) GOMV inhibits LPS-induced COX-2 and iNOS in RAW264.7 cells. RAW 264.7 cells were exposed to LPS alone or in combination with GOMV for 18 h and then Western blot was conducted using cell lysates. (B) GOMV inhibits LPS-induced COX-2 at transcription level. RAW 264.7 cells were exposed to LPS alone or in combination with GOMV for 6 h and real-time RT-PCR was conducted. The relative level of COX-2 mRNA was measured by real-time RT-PCR. Asterisks indicate statistical significance with $^{**}p<0.01$. (C) GOMV inhibits LPS-induced iNOS at transcription level. RAW 264.7 cells were exposed to LPS alone or in combination with GOMV for 6 h and real-time RT-PCR was conducted. The relative level of iNOS mRNA was measured by real-time RT-PCR. Asterisks indicate statistical significance with $^{*}p<0.05$.

GOMV suppresses oxidative damages in HaCaT cells by directly scavenging free radicals and by eliciting NRF2/ARE-dependent gene expression

To examine whether GOMV could act as a direct antioxidant, we conducted DPPH and ABTS assays. We found that

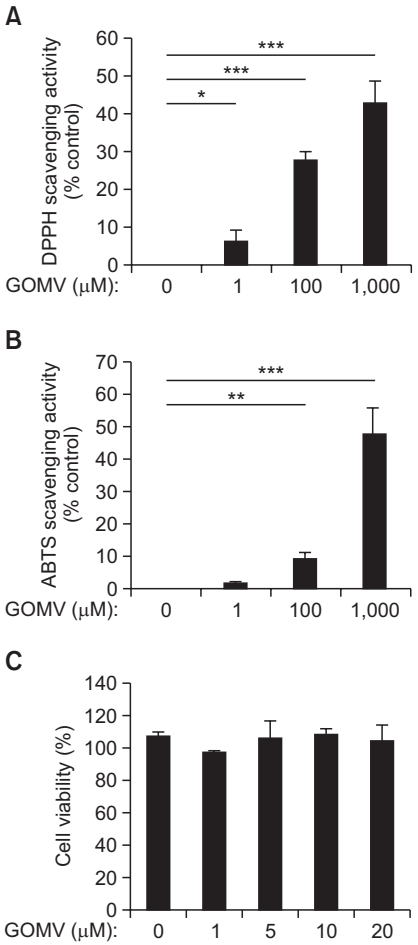

Fig. 3. GOMV directly scavenges DPPH and ABTS free radicals without affecting the viability of human keratinocyte HaCaT cells. (A) DPPH assay demonstrates that GOMV can directly scavenge DPPH free radicals *in vitro*. Asterisks indicate statistical significance with $^{*}p<0.05$, $^{**}p<0.01$ and $^{***}p<0.01$. (B) ABTS assay demonstrates that GOMV can directly scavenge ABTS free radicals *in vitro*. Asterisks indicate statistical significance with $^{**}p<0.01$ and $^{***}p<0.01$. (C) GOMV does not affect the viability of HaCaT cells. Viability was measured by MTT assay.

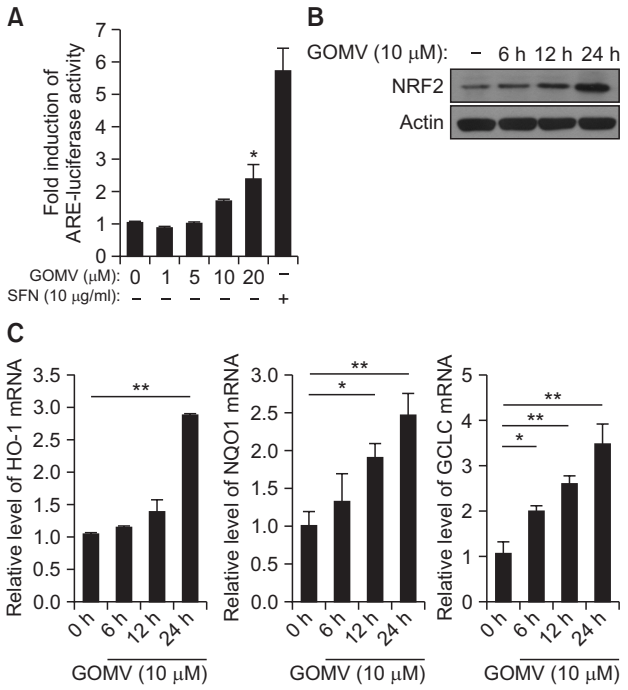

Fig. 4. GOMV activates NRF2/ARE to induce phase II cytoprotective enzymes in HaCaT cells. (A) GOMV activates ARE-dependent luciferase activity in HaCaT-ARE-GFP-luciferase cells. Sulforaphane (SFN) was included as a positive control. Asterisks indicate statistical significance with **p*<0.05, ***p*<0.01 and ****p*<0.01. (B) Western blot assay showing that GOMV induces NRF2 in HaCaT cells. (C) Real-time RT-PCR assay showing that GOMV transcriptionally activates phase II cytoprotective enzymes such as heme oxygenase-1 (HO-1, Left Panel), NAD[P]H:quinone oxidoreductase-1 (NQO1, Middle Panel), and Glutamate-Cysteine Ligase Catalytic Subunit (GCLC, Right Panel) in HaCaT cells. Asterisks indicate statistical significance with **p*<0.05, ***p*<0.01 and ****p*<0.01.

GOMV directly scavenged DPPH (Fig. 3A) and ABTS (Fig. 3B) free radicals *in vitro* without affecting the viability of human keratinocyte HaCaT cells (Fig. 3C). Besides direct detoxification of oxidants, the induction of phase II cytoprotective enzymes by NRF2 is another strategy to combat against oxidative stress in keratinocytes (Keum and Choi, 2014). To this end, we exposed GOMV to human keratinocyte HaCaT-ARE-GFP-luciferase reporter cells and measured the luciferase activity. Our results showed that GOMV significantly increased ARE-dependent luciferase activity in HaCaT cells (Fig. 4A). GOMV increased NRF2 (Fig. 4B) and NRF2-dependent phase II cytoprotective enzymes such as HO-1 (Left Panel), NQO1 (Middle Panel), and GCLC (Right Panel) in HaCaT cells (Fig. 4C). In addition, GOMV suppressed TPA-induced generation of intracellular reactive oxygen species (ROS) (Fig. 5A), and inhibited subsequent oxidative damages on nucleotides (Fig. 5B) and lipids (Fig. 5C) in HaCaT cells. Together, our results illustrate that GOMV protects keratinocytes against oxidative damages by directly detoxifying free radicals as well as by activating NRF2/ARE to induce phase II cytoprotective enzymes.

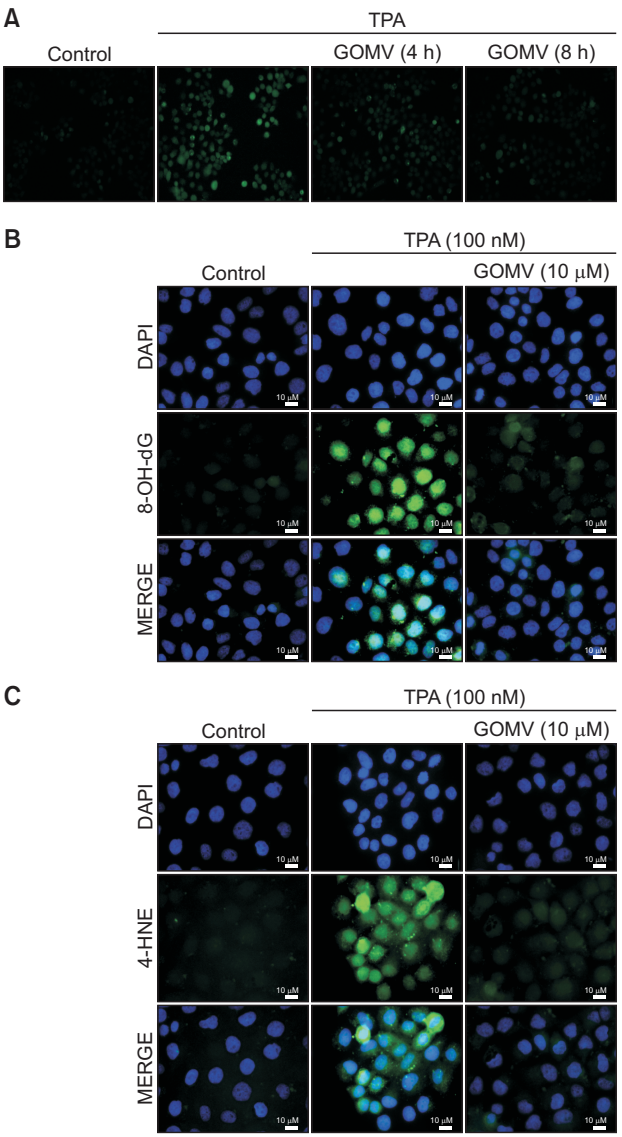

Fig. 5. GOMV inhibits TPA-induced generation of reactive oxygen species (ROS) and suppresses oxidative damages on nucleotides and lipids in HaCaT cells. (A) GOMV suppresses TPA-induced ROS generation in HaCaT cells. HaCaT cells were exposed to TPA alone (100 nM) or in combination with GOMV (10 μM). The level of ROS was observed under a fluorescent microscope after DCF-DA staining. (B) GOMV suppresses TPA-induced oxidative damages on nucleotides. HaCaT cells were exposed to TPA alone or in combination with GOMV for 24 h. The level of oxidative damage on nucleotide was monitored by staining with primary antibody against 8-OH-dG and subsequent observation under a fluorescent microscope. (C) GOMV suppresses TPA-induced oxidative damages on lipids. HaCaT cells were exposed to TPA alone or in combination with GOMV for 24 h. The level of oxidative damage on nucleotide was monitored by staining with primary antibody against 4-HNE and subsequent observation under a fluorescent microscope.

DISCUSSION

Previously, we have demonstrated that GOMV interferes with the binding between 14-3-3ε and CDK9 to suppress pro-inflammatory genes such as c-*jun* and c-*fos*, thereby attenuat-

ing mitotic progression in keratinocytes (Kang *et al*., 2014). In addition, Chang and Wu (2016) have demonstrated that GOMV exerts neuroprotective effects against focal cerebral ischemia in rats. In the present study, we provided evidence that GOMV could suppress pro-inflammatory responses in RAW 264.7 cells and inhibit oxidative damages on keratinocytes not only by directly scavenging free radicals *in vitro*, but also by activating NRF2/ARE to induce phase II cytoprotective enzymes. These results imply that GOMV possesses diverse beneficial pharmacological activities.

We have recently conducted a small-scale clinical study to examine whether hot water extract of *Saposhnikovia divaricate* exhibits anti-inflammatory effects on human skin. GOMV is a major component in *Saposhnikovia divaricate*, also known as Fangfeng in Chinese, Bangpung in Korean, and Siler in English. As a result, we found that hot water extract of *Saposhnikovia divaricata* suppressed isopropyl myristate-induced pro-inflammatory responses in the skin of human subjects without causing irritation (data not shown). Therefore, we assume that hot water extract of *Saposhnikovia divaricata* could be used for various pharmacological purposes as a source of GOMV. Presently, we are attempting to establish an optimal extraction condition to ensure that GOMV could be sufficiently extracted from hot water extract of *Saposhnikovia divaricata* without causing irritation in human skin.

CONFLICT OF INTEREST

We declare no competing financial interests.

ACKNOWLEDGMENTS

This study was supported by the Research Program of Dongguk University, 2016.

REFERENCES

Baek, S. (2011) When signaling kinases meet histones and histone modifiers in the nucleus. *Mol. Cell* **42**, 274-284.

Chang, C. Z. and Wu, S. C. (2016) 4'-O-beta-D-glucosyl-5-O-methylvisamminol, a natural histone H3 phosphorylation epigenetic suppressor, exerts a neuroprotective effect through PI3K/Akt signaling pathway on focal cerebral ischemia in rats. *World Neurosurg.* **89**, 474-488.

Itoh, K., Chiba, T., Takahashi, S., Ishii, T., Igarashi, K., Katoh, Y., Oyake, T., Hayashi, N., Satoh, K., Hatayama, I., Yamamoto, M. and Nabeshima, Y. (1997) An Nrf2/small Maf heterodimer mediates the induction of phase II detoxifying enzyme genes through antioxidant response elements. *Biochem. Biophys. Res. Commun.* **236**, 313-322.

Kang, J., Chin, Y., Lee, K., Kim, Y., Choi, B. and Keum, Y. (2014) Identification of 4'-O-beta-D-glucosyl-5-O-methylvisamminol as a novel epigenetic suppressor of histone H3 phosphorylation at Ser10 and its interaction with 14-3-3epsilon. *Bioorg. Med. Chem. Lett.* **24**, 4763-4767.

Keum, Y. and Choi, B. (2014) Molecular and chemical regulation of the Keap1-Nrf2 signaling pathway. *Molecules* **19**, 10074-10089.

Keum, Y., Kim, H., Bode, A., Surh, Y. and Dong, Z. (2013) UVB-induced COX-2 expression requires histone H3 phosphorylation at Ser10 and Ser28. *Oncogene* **32**, 444-452.

Kim, D., Lee, K., Lee, H. and Lee, C. (2002) Vitamin C equivalent antioxidant capacity (VCEAC) of phenolic phytochemicals. *J. Agric. Food. Chem.* **50**, 3713-3717.

Kim, D., Chun, O., Kim, Y., Moon, H. and Lee, C. (2003) Quantification of polyphenolics and their antioxidant capacity in fresh plums. *J. Agric. Food Chem.* **51**, 6509-6515.

Kundu, J. and Surh, Y. (2008) Inflammation: gearing the journey to cancer. *Mutat. Res.* **659**, 15-30.

Lee, J., Mailar, K., Yoo, O., Choi, W. and Keum, Y. (2018) Marliolide inhibits skin carcinogenesis by activating NRF2/ARE to induce heme oxygenase-1. *Eur. J. Med. Chem.* **150**, 113-126.

Ma, Q. (2013) Role of Nrf2 in oxidative stress and toxicity. *Ann. Rev. Pharm. Toxicol.* **53**, 401-426.

Schieber, M. and Chandel, N. (2014) ROS function in redox signaling and oxidative stress. *Curr. Biol.* **24**, R453-R462.